



Hydrology of the seas around the Sardinia, western Mediterranean

Roberto Sorgente¹, Federica Pessini¹, Aldo F. Drago², Alberto Ribotti^{1,*}, Simona Genovese³, Marco Barra⁴, Angelo Perilli¹, Giovanni Quattrocchi¹, Andrea Cucco¹, Ignazio Fontana³, Giovanni Giacalone³, Gualtiero Basilone³, Angelo Bonanno³

5 ¹Institute for the study of the anthropic impacts and sustainability in the marine environment, National Research Council, Oristano, 09170, Italy

²Institute of Energy & Transport, Malta College of Arts, Science & Technology, Triq Kordin, Paola, PLA9032, Malta

³Institute for the study of the anthropic impacts and sustainability in the marine environment, National Research Council, Capo Granitola, Campobello di Mazara, 91021, Trapani, Italy

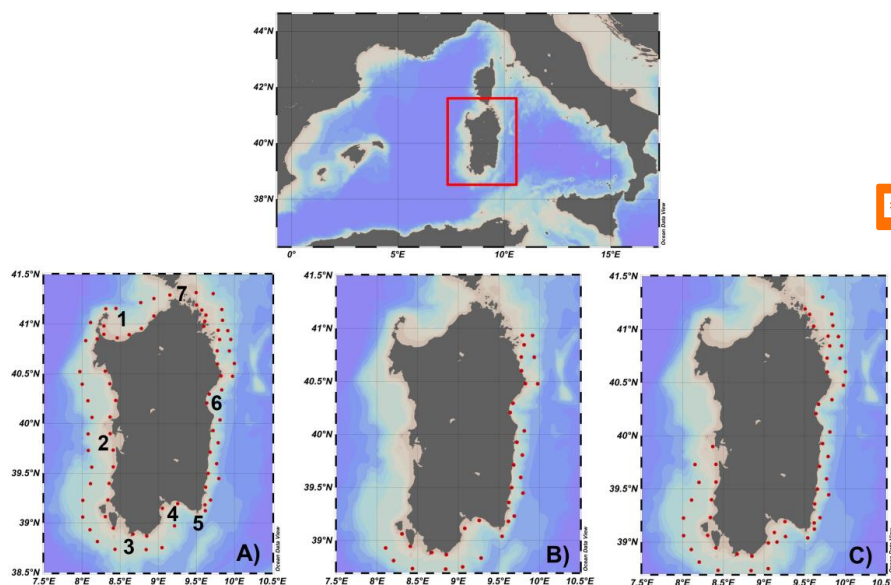
10 ⁴Institute of Marine Sciences, National Research Council, 80133, Naples, Italy

Correspondence to: Ribotti A. (alberto.ribotti@cnr.it)

Abstract. The presence and interannual variability of water masses on the continental shelf surrounding the island of Sardinia are described from three multidisciplinary cruises carried out in September 2019, late August 2020 and September 2021 in the framework of the IDMAR project. A multiparametric probe acquired CTD data along vertical profiles at a total of 166 casts located from the shelf edge to the continental slope, between the surface and 300 m depth. The analyses of these observations are for the first time identifying the water mass phenomenology on the Sardinia shelf characterized by the presence of the Atlantic Water at the surface. It shows a mild interannual variability and an unusually low salinity < 37.0 at 35 m on the south-western approaches, detected during the cruises in 2019 and 2021, and driven by the Algerian eddies. On the southern and eastern shelf, the presence of the Atlantic Water is marked by a salinity of about 38.0, and the water column is affected by the temporal and spatial variability of the South East Sardinia Gyre. These observations are opening new aspects to understand the long-term evolution of the hydrology around Sardinia in the context of the general circulation of the Western Mediterranean basin.

1. Introduction

After Sicily, Sardinia is the second largest Mediterranean island and is in the Western Mediterranean basin (Fig. 1). It is surrounded on the west by the Sardinia Sea forming part of the Algerian-Provençal sub-basin, and on the east by the deep Tyrrhenian Sea. It is separated from the island of Corsica on the north by the shallow and narrow Bonifacio Strait (point 7 in Fig. 1A) and the Gulf of Asinara (point 1 in Fig. 1A), and at the south from Tunisia by the Sardinia Channel.



30 **Figure 1: Spatial distribution of CTD casts along the coast of Sardinia as part of the cruises IDMAR2019 (panel A), IDMAR2020 (panel B), and IDMAR2021 (panel C). In panel (A) some main locations are indicated: 1) Gulf of Asinara; 2) Gulf of Oristano; 3) Cape Teulada; 4) Gulf of Cagliari; 5) Cape Carbonara; 6) Gulf of Orosei; 7) Bonifacio Strait.**

40 The width of the Sardinian continental shelf around the island varies, from a maximum of 40 km along the western coast to 5-10 km at Cape Carbonara (point 5 in Fig. 1A) on the south-east flank and around the island of Asinara on the north-west (Chiocci et al., 2021). On average its width is around 20 km. The shelf break varies in depth from 120 m at Cape Carbonara to 230 m along the western coast, being on average 150-200 m deep. Along the western and the eastern coasts, the shelf is cut by heads of canyons that usually start close to the coast and then reaching the abyssal plains.

45 The western and southern coasts of Sardinia are affected by the relatively fresh Atlantic Water (AW) by means of anti-cyclonic eddies shed by the Algerian Current (AC in Millot, 1985). These mesoscale features, named as the Algerian Eddies (AEs), are generated by baroclinic instabilities of the AC (Millot, 1987) and can transport heat content (Colas et al., 2012) as well as chemical (e.g. salt) and biological properties (e.g. nutrient and biomass, Llinas et al., 2009) impacting on climate (Wunsch, 1999) and ecological processes (McGillicuddy, 2016). AC flows eastward along the northern African coast (Millot et al., 1999; Obaton et al., 2000) and can affect the large-scale circulation (Escudier et al., 2016). AEs are large anti-cyclonic open sea eddies whose diameter varies between 50 and 250 km with their vertical extent ranging from hundreds of meters up to the sea bottom (1000-3000 m). The trajectory of AEs follows approximately a cyclonic path in the eastern Algerian basin (Fuda et al., 2000) and can cause some AW accumulated in the southern sub-basin with residence times ranging from months to years (Puillat et al., 2002; Pessini et al., 2020). They contribute to the spreading and mixing of the water masses (Millot et al., 2005) and interact with the resident Mediterranean waters at spatial scales from basin to sub-mesoscale (Puillat et al., 2002), through different mechanisms (Cotroneo et al., 2019). Due to their size and intensity, they strongly interact with the AC and can significantly modify the circulation in the region (Millot, 1987; Taupier-Letage and Millot, 1988). Then, due to the transportation of the AW, AEs contribute to the formation of the North Balearic Front (Fuda et al., 2000; Olita et al., 2014; Seyfried et al., 2019; Barral et al., 2021). This front forms a Lagrangian barrier (Mancho et al., 2008) that separates the circulation of the Algerian basin from the mean cyclonic circulation in the northern Provençal through the Western Mediterranean Current (WMMC in Pinardi et al., 2015). WMMC is an eastward-wide meandering free jet, flowing approximately at 39.5°N, that exhibits a significant seasonal variability (Garcia et al., 1994), reaching the Sardinia Sea in winter at its southernmost position (Pessini et al., 2018). Here the WMMC takes the name of Southerly Sardinia Current (SSC



in Pinardi et al., 2015) and it can interact with the AEs affecting the water masses and the surface circulation offshore the coast (Ribotti et al., 2004). Furthermore, the western coast of Sardinia is also affected by upwelling events triggered by the wind forcing (Olita et al., 2013).

The eastern and southern coasts of Sardinia overlook the Tyrrhenian sub-basin, the deepest area of the western Mediterranean with its 3785 m maximum depth. Here the circulation is driven by local atmospheric forcing and by water exchanges occurring at the Sardinia, Corsica, and Sicily channels (Artale et al., 1994), characterised by very relevant mesoscale dynamics (Vetrano et al., 2010). The main dynamical features are the Northern Tyrrhenian Gyre (NTG), the South West Tyrrhenian Gyre, also known as South East Sardinia Gyre (SESG in Sorgente et al., 2003), and the South East Tyrrhenian Gyre (SETG in Pinardi et al., 2015), consistent with classical pictures of the geostrophic circulation from Krivosheya and Ovchinnikov (1973). The NTG drives the circulation in the northern part of the Tyrrhenian Sea by permanent dynamic structures like the wind-induced dipole known as the Bonifacio Gyre (Artale et al., 1994). It is centred just east of the Bonifacio Strait, represented by a cyclonic structure in the north coupled with a smaller anti-cyclonic gyre companion to the south, both exhibiting a strong seasonal variability (Iacono et al., 2021). It could affect the circulation and the hydrological characteristics on the Sardinia continental slope, but there is no evidence of this. The SETG is feeble in its mean because the south-eastern Tyrrhenian Sea is an area of frequent anti-cyclonic eddies that weaken the cyclonic mean circulation (Rinaldi et al., 2010). The SESG is in a wide area of sea between Sardinia and Sicily, already present in the circulation scheme of Krivosheya (1983).

Yearly hydrological surveys, between 2019 and 2021, were conducted in the coastal seas around Sardinia by the Italian National Research Council (CNR) under the framework of three cruises named IDMAR2019, IDMAR2020 and IDMAR2021, all conducted at the end of the summer season. The novelty of these three cruises, compared to the past, is that previous cruises with casts on the Sardinian shelf were mainly limited to the west (Onken et al., 2018; Ribotti et al., 2019a,b, 2022) and south of Sardinia (Ribotti et al., 2004). The analyses of these new data provide a first complete picture of the Sardinian coastal hydrology, identifying the thermodynamic differences between the coasts around Sardinia and the spatial and inter-annual variability of the properties of its water masses. The document also provides contributions that may allow the modellers to assess the performance of hydrological models on this coastal area.

The cruises and the collected data are described in section 2 followed by their analyses and interpretation for the study area in section 3. Section 4 draws the conclusions.

2. Data and Methods

Three oceanographic cruises, named IDMAR, were carried out around the coastal shelf of Sardinia during the late summer from 2019 to 2021. Cruise data are shown in Table 1.

The weather conditions during the first cruise featured calm seas and weak winds while during the second and third cruise the weather was unstable with westerly winds > 10 m/s, strongly conditioning the sampling.

Name cruise	Start time	End time	No. of CTD casts
IDMAR2019	September 2, 2019	September 15, 2019	77
IDMAR2020	September 26, 2020	October 8, 2020	34
IDMAR2021	August 28, 2021	September 5, 2021	54

Table 1: The columns indicate the name of the cruise, the start and end of observation campaign, and the number of CTD casts.

The in-situ sampling design focused on the shelf, between the near-shore in very shallow water and the continental slope, with transects approximately perpendicular to the coast. Each transect was composed of two CTD stations spaced between 13 and 29 km, depending on the shelf's width. Casts on the slope were anyway limited to a maximum depth of 300 m, regardless of



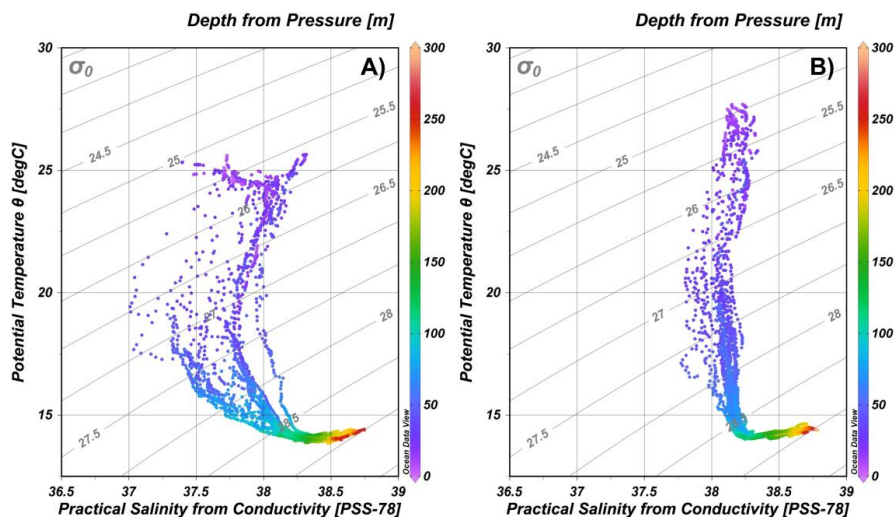
95 the real depth of the bottom. During each cruise (Fig. 1) high-resolution vertical profiles of temperature and salinity were
acquired at each hydrological station using a previously calibrated Sea Bird Electronics multiparametric probe, model SBE
911 plus, on the CNR R/V G. Dallaporta. The CTD was mounted on a General Oceanics Rosette system and equipped sensors
of conductivity, temperature, depth, and dissolved oxygen which sampled the hydrological parameters along the vertical at 24
100 Hz and with a lowering speed of 1ms-1. These data were respectively measured by means of: a SBE 4 water conductivity
sensor, with a resolution of 3×10^{-4} Sm-1 and accuracy of ± 0.0003 S/m; a SBE 3F thermometer, with a resolution of 0.00015
°C/bit at -1 °C or 0.00018 °C/bit at 31 °C and accuracy of ± 0.001 °C; a Paroscientific Digiquartz pressure sensor with $\pm 0.015\%$
of full scale range of accuracy; a SBE 43 polarographic membrane sensor for dissolved oxygen with a range of 120% of surface
saturation and an accuracy of $\pm 2\%$ for saturation. After their acquisition, data were processed to delete spikes and low-quality
data, using the SBE Data Processing™ software, a specific SBE software that permits also to align all sensors along the profile
105 due to a different time response of each sensor followed by a control of each profile to highlight further bad data. Then
potential temperature, practical salinity (hereafter salinity), and potential density anomaly were calculated and plotted using
the Ocean Data View software by Schlitzer (2023). In support of temperature and salinity vertical profiles, Absolute Dynamic
Topography (ADT) fields were used from satellite data from the Copernicus Marine Service (CMEMS; Mediterranean Sea
gridded L4 sea surface heights and derived variables reprocessed. E.U. Copernicus Marine Service Information (CMEMS,
110 Marine Data Store (MDS). DOI: 10.48670/moi-00141. Last access on 22 Sept. 2023). These fields were estimated by Optimal
Interpolation, merging the L3 along-track measurements from the different available altimeter missions on a horizontal
resolution of $1/8^\circ \times 1/8^\circ$. The geostrophic currents were obtained from SLA and ADT by assuming a geostrophic balance.

3. Results and Discussion

The characteristics of the different type of water masses and their interannual variability are specified below distinguishing
115 between ranges and core values of potential temperature (hereafter temperature, T), practical salinity (hereafter salinity, S) and
potential density anomaly (hereafter density, sigma).

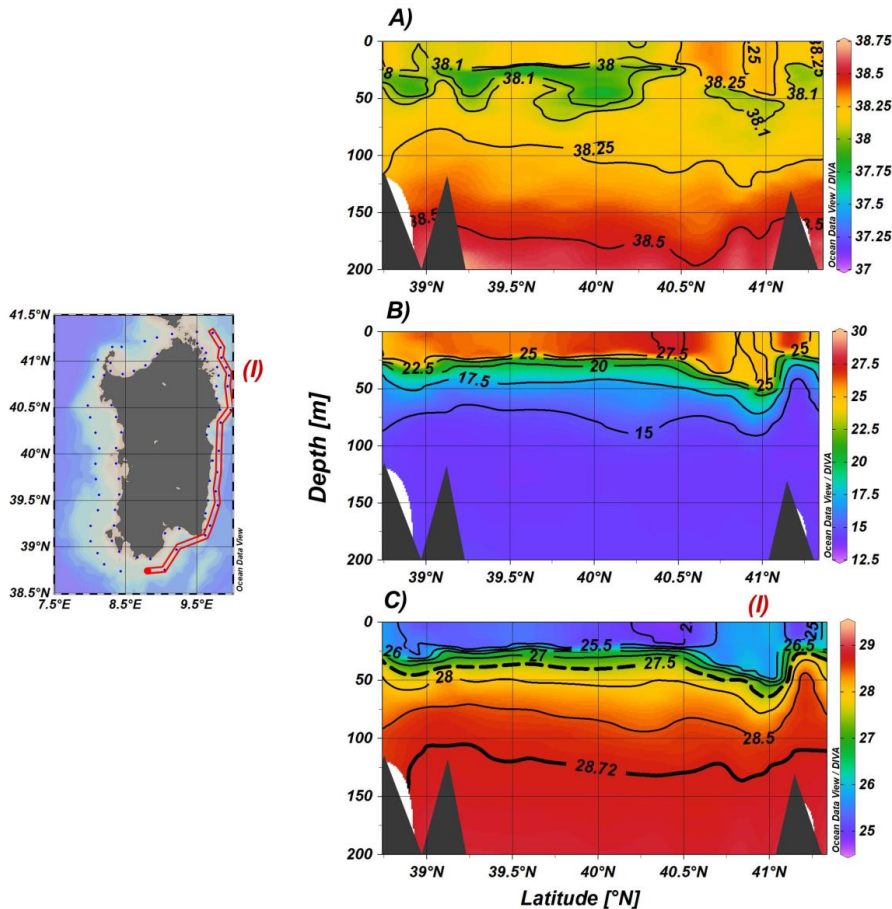
3.1 The cruise IDMAR 2019

The spatial distribution of CTD casts (2-15 September 2019) is shown in Fig. 1A, providing a quasi-synoptic view of the
coastal thermohaline characteristics of the water masses all around Sardinia. The TS diagram for the vertical profiles carried
120 out along the western and eastern coasts shows the water column affected by the AW (Fig. 2). The water column is well
stratified, indicating the progressive mixing between the AW and the saltier waters of the coastal area.



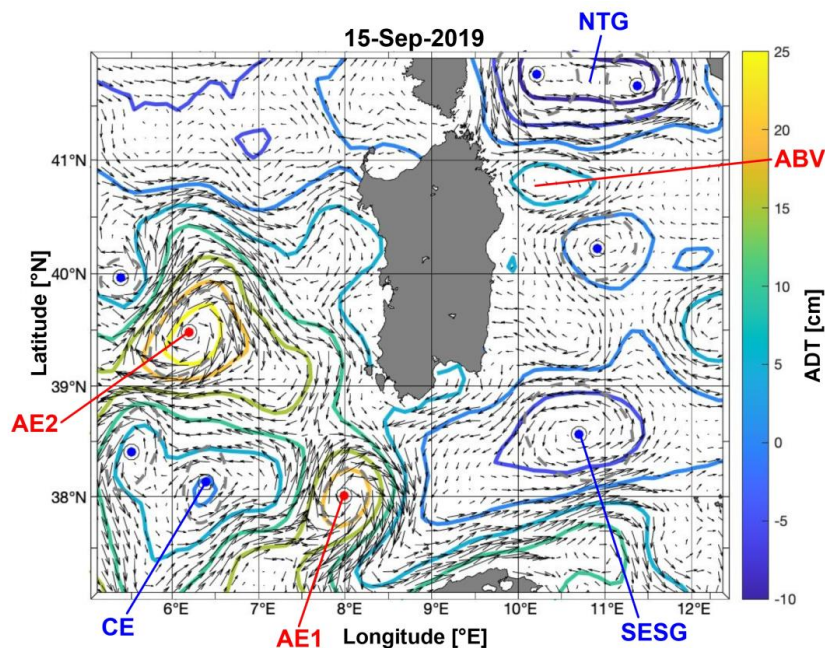
125 **Figure 2: T-S diagrams of the western (panel A) and eastern (panel B) coast of Sardinia during IDMAR 2019. All depths from 5 m to the bottom are considered. Colours show the depth [m].**

130 Along the western coast (Fig. 2A) the temperature ranged from 26 °C at the surface to 14 °C at the deepest depth (hereafter mentioned as bottom, for simplicity), while the salinity ranged from a minimum of about 37.00 to a maximum of 38.66, again measured up to the deepest point of the casts. The core of the AW, characterized by its salinity minimum, hereafter named as fresh AW, was located at a water depth defined by a density of 26.451 kg m⁻³. This unusual low salinity was observed at 35 m in correspondence of the casts in the southwestern domain (Fig. 3A).



135 Figure 3: Vertical distribution of salinity (A), potential temperature (B in $^{\circ}\text{C}$) and potential density anomaly (C in $[\text{kg m}^{-3}]$) along the western shelf of Sardinia (left panel) from the external casts in the upper 200 m. The isopycnal 28.72 Kg m^{-3} (the bold black line) represents the deepest boundary of AW as defined by Knoll et al. (2017), while 27.5 kg m^{-3} is the deepest limit of the fresh AW.

140 Recently Knoll et al. (2017) observed salinities lower than 37.2 at the surface in June 2014 in the same area. Also, Ribotti et al. (2004) measured similar values in correspondence of two AEs located offshore the western Sardinian shelf during the cruise MedGOOS4 in May 2002, as Benzohra and Millot (1995) and Taupier-Letage et al. (2003) in the eastern part of the Algerian Basin. Signatures of fresh AW are observed also on the northernmost Sardinian shelf, characterised by a wide surface layer covering the upper 60 m, while the AW affects the whole water column up to about 150 m. The vertical distribution of potential temperature is shown in Fig. 3B. The field is characterized by a homogeneous upper layer with a superficial temperature of about 25°C along the whole transect. This layer extends vertically from the sea surface to about 40 m depth. Below this layer, 145 the potential temperature decreases forming a wide thermocline layer. The mixed layer depth remains approximately constant above 40°N , while below it waves reaching the maximum depth of 50 m. The corresponding density field is represented in Fig. 3C, which shows the impact of AW in the surface layer. In order to identify the possible causes of these anomalous absolute minima, the Absolute Dynamic Topography and geostrophic velocities are shown in Fig. 4.



150

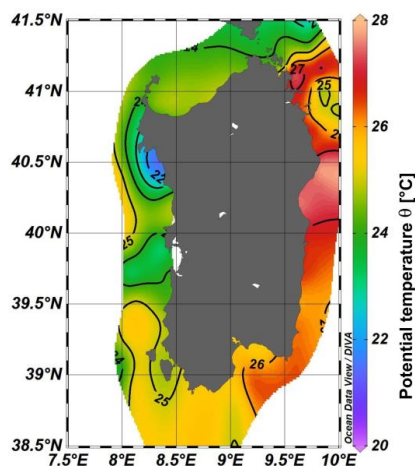
Figure 4: Absolute Dynamic Topography contours overlaid with geostrophic currents for September 15th 2019. Magenta lines, every 5 cm contours, represent the border of the anticyclonic structures while blue lines represent the border of the cyclonic ones. The dashed lines represent the separation zones between cyclonic and anticyclonic areas.

155

This figure identifies the Sardinia Sea as an energetic area characterized by several mesoscale features. As described by Puillat et al. (2002), the mesoscale features represent baroclinic instabilities of the AC, which circulate cyclonically within a gyre in the Algerian Basin. The interaction between the anti-cyclonic AE1 (about 100 km), which is constrained by the SESG on the east, and the large cyclonic eddy (CE) on the west, contributes to the spreading of the AW directly from the Algerian coast to the south-western Sardinian shelf, modifying the water properties of the surface water column with less saline water (about 37.00). The largest and northern anticyclonic eddy AE2 (about 200 km in extent) could be affected by the circulation on the western Sardinia shelf, spreading AW (about 37.5) from the centre of the Algerian Basin toward the coast. These signatures of AW affected only the external CTD casts on the shelf break, till 250 m depth, while the salinity increased below the halocline and toward the coast (not shown). In the north-west, a small signature of superficial coastal upwelling was captured in the shallowest coastal casts, inducing an evident decrease of the sea surface temperature to about 21 °C. Respect the offshore, the

165

sea surface gradient temperature is about +3 °C (Fig. 5).

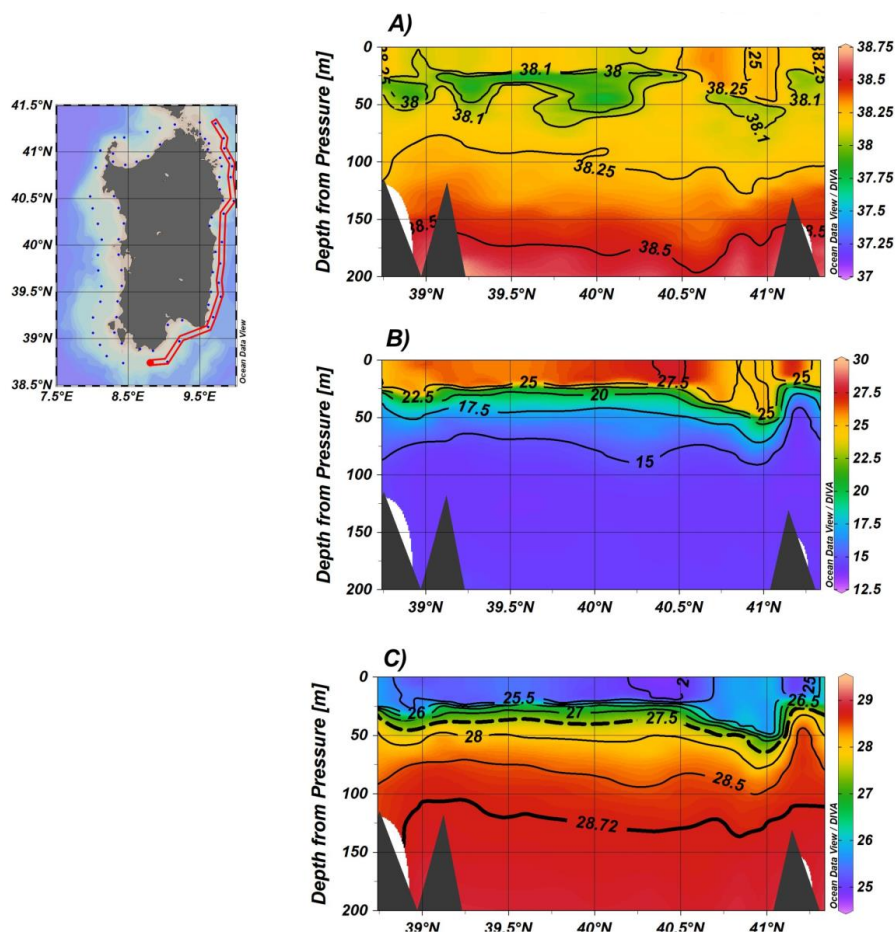


170 **Figure 5. Map of sea surface temperature.** The north-western upwelling was measured by the casts carried out on September 13th 2019.

This process was analysed through a numerical study, which found that wind direction and current intensity could participate to precondition and enhance upwelling (Ribotti et al. 2004; Olita et al., 2013). The footprint of such a preconditioning has a clear SST signature in thermal satellite images, showing lower coastal values compared to offshore (not shown). No upwelling

175 was evident in the southwestern Sardinia shelf, even if it was reported by Olita et al. (2013).

Along the eastern flank of Sardinia, the TS diagram (Fig. 2B) shows a lower variability in terms of salinity compared to the western side. The salinity ranged between the minimum of 37.77 and 38.78 at the bottom, while the temperature between 14.8 °C at the bottom and a maximum of 28 °C at the surface. The core of fresher AW of about 38.0 was at 20-45 m (Fig. 6A).



180

Figure 6. Vertical distribution of salinity (A), potential temperature (B in $^{\circ}\text{C}$) and potential density anomaly (C in kg m^{-3}) along the southern and eastern shelves observed from the external casts in the upper 200 m. The isopycnal 28.72 Kg m^{-3} (the bold black line) represents the lowest boundary of AW as defined by Knoll et al. (2017), while 27.5 kg m^{-3} is the deepest limit of the fresh AW.

185

The vertical distribution of potential temperature detects a thinner homogenous superficial layer characterized by a sea surface temperature of about 25°C , while between the parallels $40\text{--}40.75^{\circ}\text{N}$, the sea surface temperature is between $27.5\text{--}30^{\circ}\text{C}$. Below the superficial layer, a sharp thermocline is detected that extends vertically approximately from 30 m depth, except on the northern side where it sinks to 50 m and then rises to 20 m (Fig. 6B). Unlike the spatial distribution of salinity field, the potential temperature strongly determines the density field (Fig. 6C). It shows the net separation between the thin surface layer

190

of light waters, slightly affected by signatures of AW, and the deeper layer by saltier and colder waters. The weak signatures of AW could be due to the influence of the SESG circulation (see Fig. 4) that appears as a wide and cyclonic gyre extending into the centre of the Tyrrhenian basin. Its horizontal circulation diffuses the relatively fresh AW from the southern side of the Sardinia Channel and flows cyclonically, weakly affecting the resident water masses offshore along the central-southernmost shelf. On the contrary, highest salinity values of about 38.3 were observed north-east of Sardinia where casts were realised 7

195

days before the previous ones (the stop was necessary due to bad weather conditions). Highest values of sea surface temperature were measured in the central side of the eastern Sardinian coast (not shown) up to 28°C , about 3°C higher than on the western coast. The vertical distribution of the potential density anomaly field is shown in Figure 6B, showing a rising isopycnal from



50 m depth toward the surface in the northern side of domain. This could be due to the interaction of the coast with the NTG, also better known as Bonifacio Vortex, and its coupled anti-cyclonic Bonifacio Vortex (hereafter as ABV), as described by Perilli et al., 1995.

200

3.2 The cruise IDMAR 2020

This cruise was carried out from 26 September to 8 October 2020 (Tab. 1) on the eastern and south-western shelves of Sardinia (Fig. 1B), while the western shelf was not monitored. The relationship between temperature and salinity for the south-western and eastern continental shelves are shown in Figs. 7A and 7B.

205

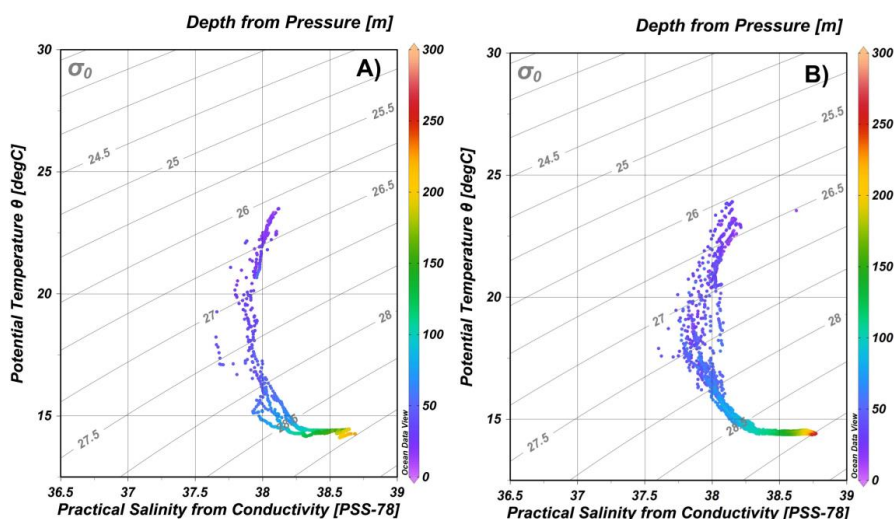


Figure 7. T-S diagrams of the western (panel A) and eastern (panel B) Sardinian shelf during IDMAR 2020. As shown in Figure 1B, the central-western and north-western domains were not monitored. All depths from 5 m to the bottom are considered. Colours show the depth [m].

210

The water columns detect similar water properties with potential temperatures ranging from 24 °C at the surface to 14.8 °C at the bottom, while salinity from a minimum of 37.66 to a maximum of 38.7 at the bottom. The core of the AW is higher than in the previous cruise and it was observed at about 40 m, only in correspondence of casts in the south-west domain and at the centre of the eastern coast (Fig. 8A).

215

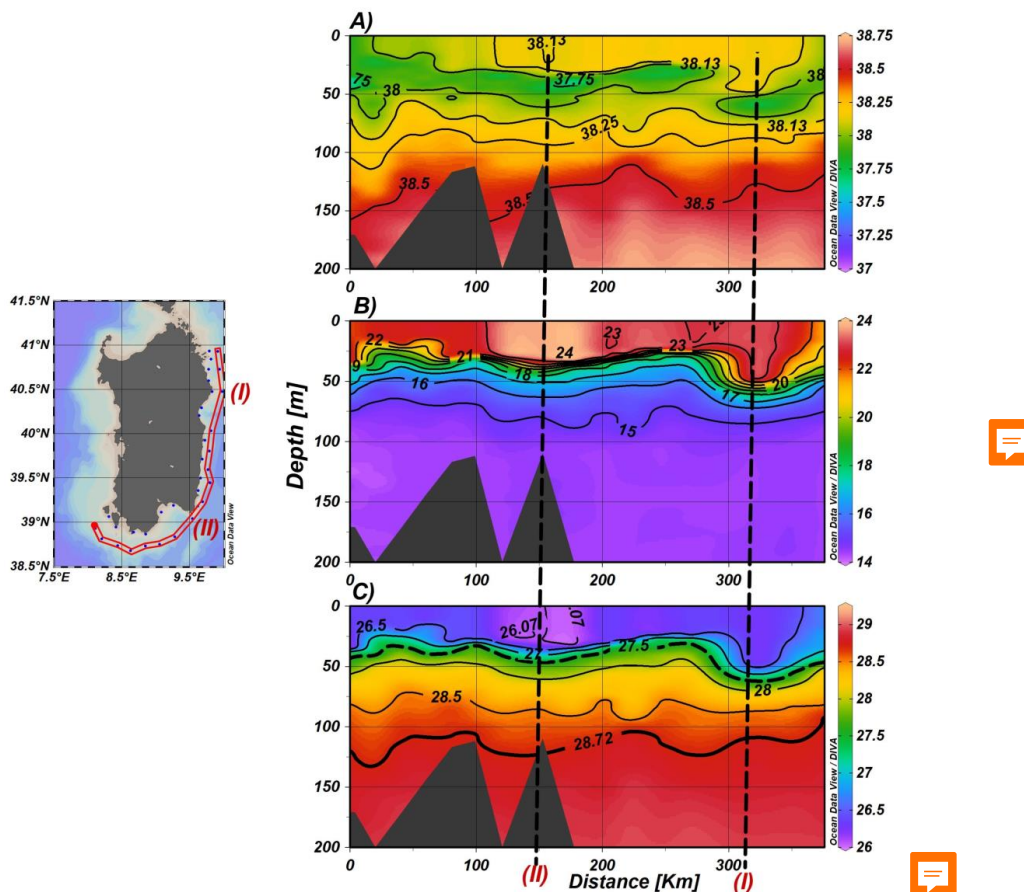
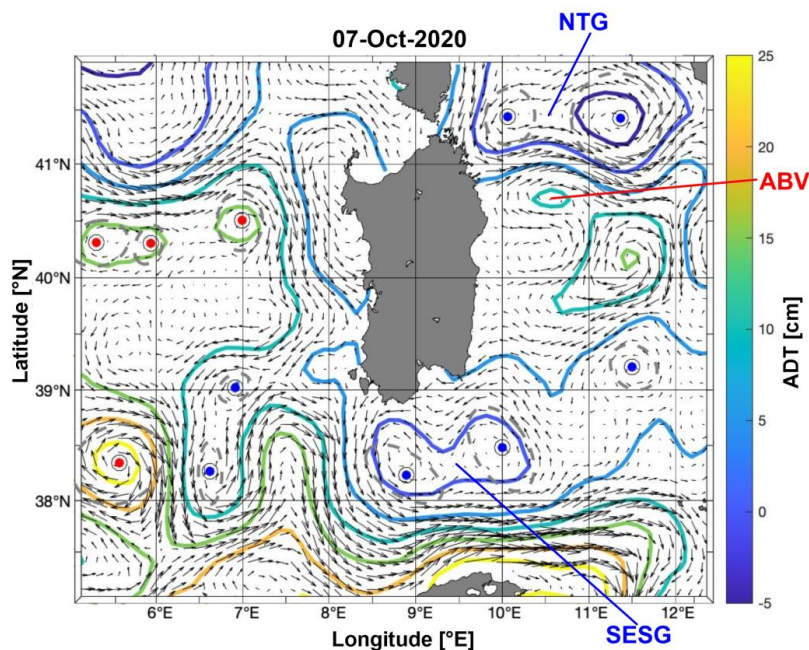


Figure 8. Vertical distribution of salinity (A), potential temperature (B in $^{\circ}\text{C}$) and potential density anomaly (C in kg m^{-3}) along the southern and eastern shelves observed from the external casts in the upper 200 m.

220 However, a sub-surface layer of AW is observed between 30-55 m depth. The impact of the AW is more evident than in the previous cruise (IDMAR 2019), affecting almost the whole transect, also in the northern casts. Here, the AW sinks up to 70 m forming part of a homogeneous surface thermal layer (Fig. 8B) where the temperature is about 23°C . The shape of isotherm highlights a signal of downwelling near the coast. The thickness of this surface layer decreases from the sea surface to 45 m depth towards south. Inside this superficial layer the temperature is approximately constant, except between 100-200 km, where warm water is observed with a maximum temperature of about 24°C . Below this superficial layer, the temperature decreases monotonically up to a depth of 75 m, forming a sharp thermocline layer. Further down, the temperature remains approximately constant with increasing depth. The correspondent density field is shown in Fig. 8C. It shows the net separation between the thin surface (about 45 m) of lighter waters affected by the AW and the deeper layer characterised by saltier and colder waters, approximately from 55 m to the bottom. From the analyses of the Absolute Dynamic Topography and geostrophic currents (Fig. 9), the signatures of the observed AW could be again due to the influence of SESG circulation. With respect the previous cruise, the SESG appears displaced westward. Its circulation could have forced the transport of AW from the Tunisian shelf towards Sardinia and hence affecting the CTD casts in the south-western domain and along the eastern coast. In the northern side a signal of downwelling is detected and it could be due to the impact of the ABV with the coast.



235

Figure 9. Absolute Dynamic Topography contours and geostrophic currents on October 7th 2020. Magenta lines represents 5 cm contours. Cyclonic and anticyclonic eddy centres, obtained by the Eddy detection and tracking algorithm, are indicated respectively by blue and red points.

240 3.3 The cruise IDMAR 2021

The cruise was carried out from 28 August to 5 September 2021 (Tab. 1) on the south-western and the whole-eastern Sardinian shelves (Fig. 1C). The TS diagrams for the two above mentioned shelves (Figs. 10A and 10B, respectively) show the water column mainly affected by the superficial AW, by a strong vertical stratification and the progressive mixing with the saltier coastal waters.

245

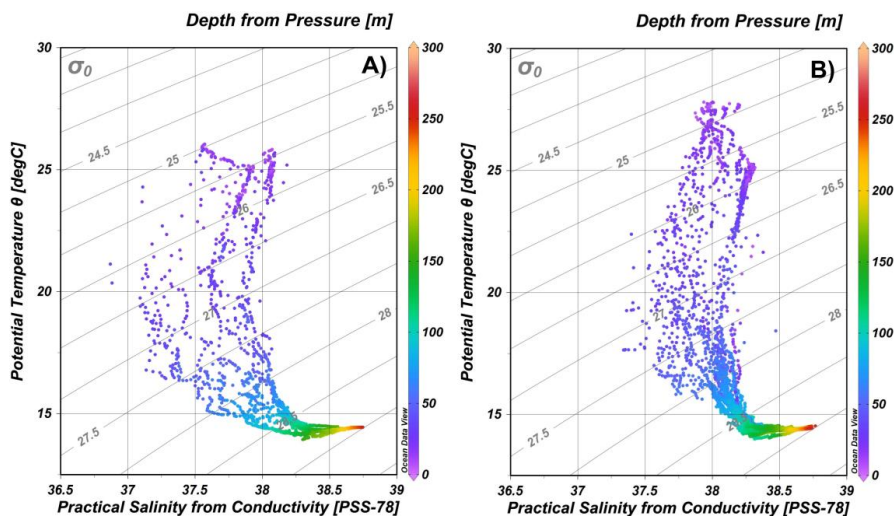
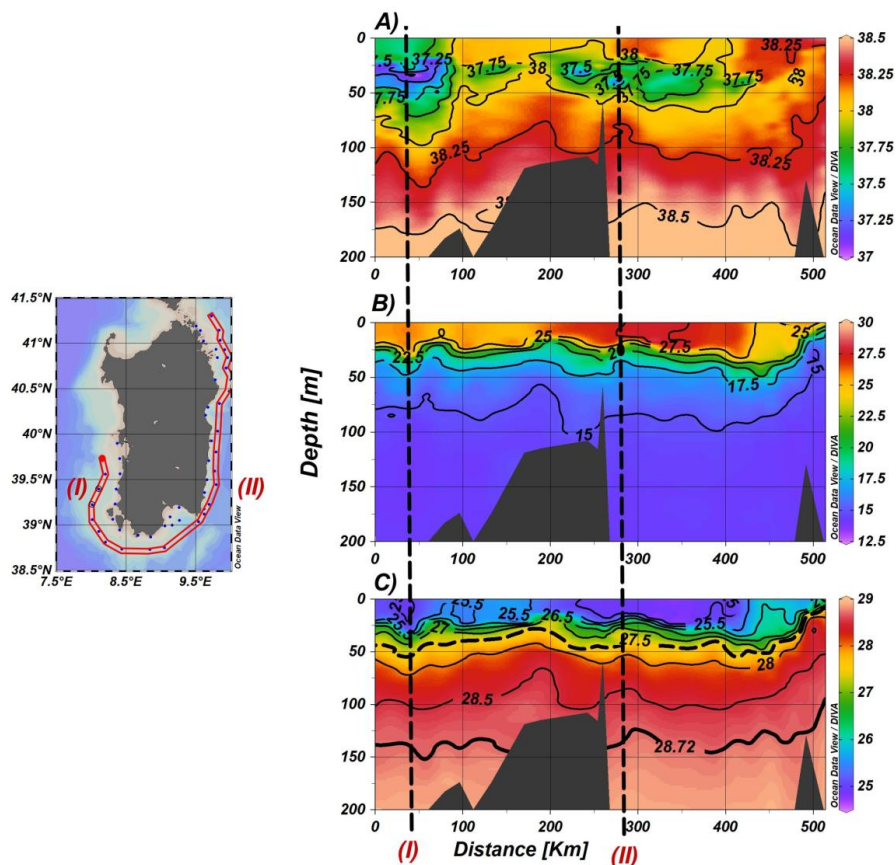




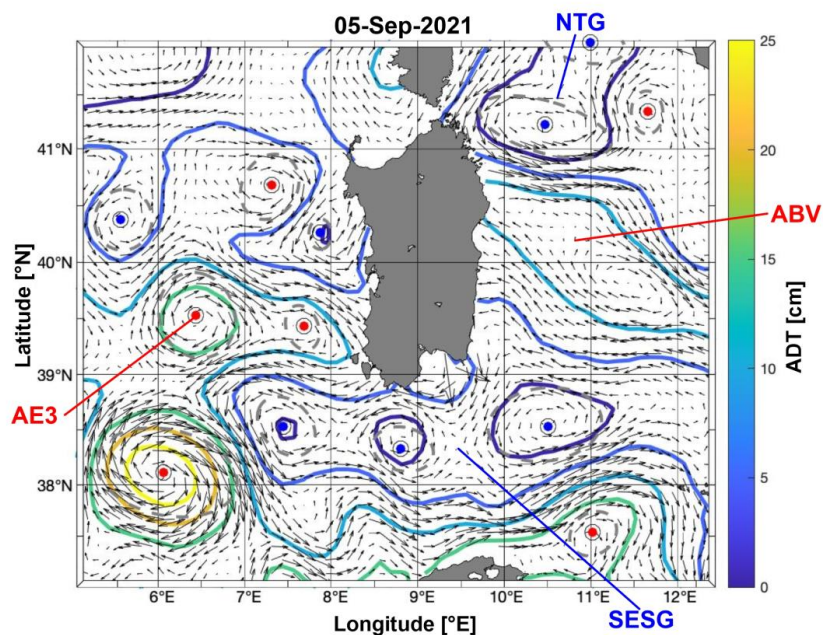
Figure 10. T-S diagrams of the western (panel A) and eastern (panel B) Sardinian shelf during IDMAR 2021. All depths from 5 m to the bottom are considered. Colours show the depth [m].

250 The diagram shows the core of the AW characterized by a minimum of salinity of 36.87 at 33 m in the south-western casts (Fig. 11A).



255 Figure 11. Contour plots showing the upper 200 m of the vertical distribution of salinity (panel A), potential temperature (B in [°C]) and potential density anomaly (C in [kg m⁻³]) from the CTD casts during IDMAR 2021.

This unusual low value of salinity (density = 25.89 kg m⁻³) was also observed during the cruise in 2019 (see Fig. 2A) and could represent the spreading of fresh AW induced by the large anti-cyclonic AE3 circulation (Fig. 12).



260

Figure 12. Absolute Dynamic Topography contours and the geostrophic currents on September 5th 2021. Magenta lines represent 5 cm contours. Cyclonic and anticyclonic eddy centres, obtained by the Eddy detection and tracking algorithm, are indicated respectively by blue and red points.

265

Due to its position and horizontal dimension, the AE3 could transport the fresher AW from the central Algerian basin toward the coast affecting the water column with lower salinity waters (mean values of 37.25) observed by the CTD casts over the south-western shelf. Other signatures of fresh AW (with higher values of salinity core of about 37.5) are observed also along the east-southern Sardinia shelf. This signature appears more evident than during the previous cruises in 2019 and 2020 (see Figs. 6A and 9B, respectively).

270

As described in the two previous paragraphs, they could represent the impact of sub-superficial veins of fresh AW that re-circulate into the Sardinia Channel forced by the SESG (Fig. 12). Here, SESG is a wider and more intense gyre than in the previous years, extending westward until the 7°E. Moreover, this feature is formed by three sub-cyclonic eddies than can transport the fresh AW toward the Sardinian continental shelf. Induced by the sub-cyclonic eddies, these veins of fresh AW could affect the water column properties of the casts over the southern and eastern Sardinia shelves,

275

as shown in Figs. 11A and 11B. The sub-surface layer of AW, which involved most of the meridional transect, was below the upper 30 m layer characterized by a warmer water with a maximum temperature of about 27.5 °C (Fig. 11B). Its maximum vertical extension was in correspondence of the casts located in the south-eastern casts, where the thermocline reached a depth of about 40 m. Away from this warmer area, the mean thermocline depth decreased slightly. Below the thermocline the temperature remains approximately constant with depth. The corresponding density field is shown in Fig. 11C, showing again the separation between the thin surface layers of light waters, fresher and warmed, and the deeper layer characterized by saltier and colder waters.

280

The northern casts also detect a gradual rise of the isopycnals (and isotherms) up to the sea surface. This could be due to the interaction of the MAV circulation with the north-eastern coast of Sardinia.



3.4 Interannual variability

The IDMAR datasets presented in the previous section are used to characterize the interannual variability of the water masses. Mean values of temperature, salinity and density are calculated for the west coast (longitude <math><9.0^\circ\text{E}</math>) and eastern coast (Longitude > S_{\min}), potential temperature ($T_{S_{\min}}$), density ($\sigma_{S_{\min}}$), all taken at the depth of S_{\min} ($H_{S_{\min}}$). Unfortunately, no previous CTD data in the two areas are available to be used for comparison. Considering the full water column the interannual variability in potential temperature, salinity, and density is small on both the western and eastern coasts. These changes in the mean potential temperature, salinity and density are summarised in Table 2.

Years	Western coast				Eastern coast			
	N. of stations	Temp. Std	Sal. Std	Dens. Std	N. of stations	Temp. Std	Sal. Std	Dens. Std
2019	29	17.08 4.46	38.108 0.304	27.816 1.274	55	17.27 4.09	38.324 0.395	27.925 1.217
2020	9	17.00 3.30	38.184 0.326	27.916 1.011	25	16.69 3.39	38.338 0.277	28.114 1.002
2021	18	17.14 4.16	38.085 0.332	27.791 1.247	35	17.03 3.94	38.281 0.407	27.961 1.218

Table 2: Mean values of potential temperature [$^\circ\text{C}$], salinity, density [kg m^{-3}], and standard deviation (Std) estimated for the full water column (0-300 m) on the two coasts for the three cruises.

From 2019 to 2021 the mean potential temperature taken over the three years ranged between 17.07°C and 16.99°C on the western and eastern coast, respectively, while the mean salinity between 38.125 and 38.314 . The mean salinity was always over 38.0 , while lowest values of about 38.085 are consistently observed on the western coast in August 2021. The highest value of 38.338 was on the eastern coast in 2020. The highest density was $>28.0 \text{ kg m}^{-3}$ in 2020 on the eastern coast, due to the decrease of the sea surface temperature with a mean value of about 16.69°C induced by the heat loss in September (not shown).

In order to estimate the significance of the inter-annual variability of the AW, we considered the salinity minimum S_{\min} . On the western coast the mean value of S_{\min} varied between 37.538 in 2021 to 37.877 in 2020 (Table 3). On the eastern coast, S_{\min} ranged between 37.808 in 2021 to 38.038 in 2019. The latter value represents the highest value of S_{\min} observed during the three cruises, while the absolute lowest value of 37.538 is observed in 2021 on the western coast. On the same coast, the mean potential temperature at the depth of the S_{\min} ($T_{S_{\min}}$, Table 3) varied between 19.83°C in 2020 to 20.90°C in 2021. On the eastern coast, $T_{S_{\min}}$ ranged between 19.55°C in 2020 to the maximum of 21.09°C in 2019. Another important parameter is the mean depth of the S_{\min} ($H_{S_{\min}}$, Table 3) for both coasts; this was about 31 m with a mean standard deviation at 11.6 m . More precisely, $H_{S_{\min}}$ ranged between 27.84 m in 2021, and 33.74 m in 2020 on the western coast, and between 30.74 m in 2019, and 32.78 m in 2020 on the eastern coast. The highest and the lowest values of $H_{S_{\min}}$ were observed along the western coast.

Years	Western coast					Eastern coast				
	N. stations	S_{\min} Std	$T_{S_{\min}}$ Std	$H_{S_{\min}}$ Std	$\sigma_{S_{\min}}$ Std	N. stations	S_{\min} Std	$T_{S_{\min}}$ Std	$H_{S_{\min}}$ Std	$\sigma_{S_{\min}}$ Std
2019	29	37.650 0.276	20.37 2.59	30.18 12.50	26.660 0.694	55	38.038 0.113	21.09 2.45	30.74 13.39	26.764 0.651
2020	9	37.877	19.83	33.74	26.995	25	37.899	19.55	32.78	27.083



		0.104	1.60	9.46	0.378		0.132	1.83	13.81	0.423
2021	18	37.538	20.90	27.84	26.450	35	37.808	20.73	31.27	26.675
		0.335	1.48	7.11	0.485		0.249	3.01	13.37	0.8440

315

Table 3: Mean values of potential temperature [°C], salinity, density [kg m⁻³], depth [m], and standard deviation (Std) calculated at the salinity minimum S_{min} on the two coasts for the three cruises.

The interannual variability of S_{min} between 2019 and 2021 is very mild, with average values of 37.69 (Std of about 0.24) on the western coast, and 37.91 (Std of about 0.16) on the eastern coast. The mean potential temperatures at S_{min} were similar along both coasts. T_{Smin} ranged around the mean value of 20.4 °C with an Std at about 2.16 °C, as well as the mean depth of S_{min}. We can then consider the impact for the AW on the two coasts not to be significantly different (Fig. 13).

320

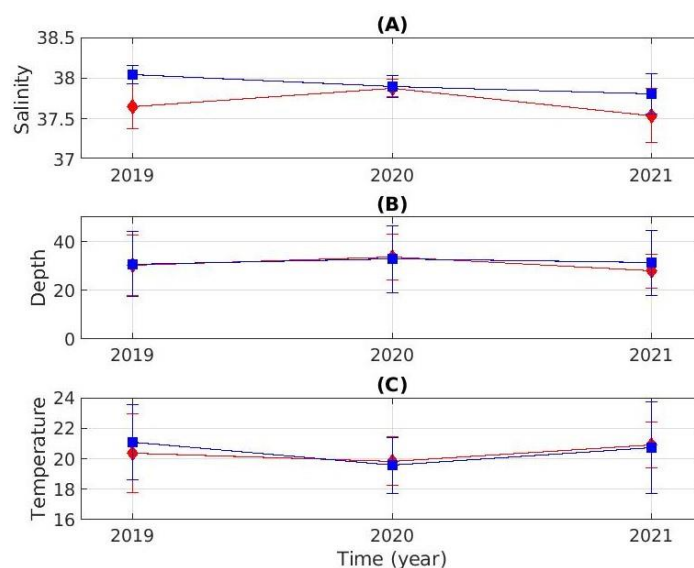


Figure 13. Interannual fluctuations in the mean values of minimum salinity (panel A), mean depth (panel B in [m]) and mean potential temperature (panel C in [°C]) both at minimum of salinity observed from 2019 to 2021 on the western coast (red line) and eastern coast (blue line). The circles indicate the mean value and the bars show the standard deviation.

325

As expected, the interannual variability is higher in the mixed layer (0-20 m), especially in terms of sea surface temperature which is influenced by different atmospheric forcings and conditions during different phases in which the cruises were conducted. On the western coast, the mean sea surface temperature ranged between 22.62 °C in 2020 and 24.76 °C in 2021, while the variation on the eastern coast ranged between 22.65 °C in 2020 and 27.89 °C in 2019, the latter value being the highest observed during the IDMAR cruises, while the lowest mean sea surface temperature was in 2020 on both coasts, when the cruise was carried out in the beginning of autumn. For both areas, the mean standard deviation is about 7.77 °C for the western coast, while it is 8.63 °C for the eastern coast.

330

Western coast					Eastern coast			
Years	N. of stations	Temp. Std	Sal. Std	Dens. Std	N. of stations	Temp. Std	Sal. Std	Dens. Std
2019	29	24.30	37.909	25.751	55	25.89	38.217	25.496
		8.29	0.393	2.397		9.64	0.239	2.726
2020	9	22.62	38.028	26.345	25	22.65	38.114	26.399
		6.51	0.277	1.840		6.76	0.364	1.971
2021	18	24.76	37.872	25.586	35	25.63	38.099	25.475
		8.51	0.414	2.494		9.49	0.324	2.760

Table 4: Mean values of potential temperature [°C], salinity, density [kg m⁻³], and standard deviation (Std) estimated at the mixed layer on the two coasts for the three cruises.

335



4. Summary and conclusions

CTD casts collected around Sardinia during three dedicated oceanographic cruises carried out in late summer between 2019 and 2021 (Tab. 1) have been analysed. Results show that AW affects the water column up to approximately the upper 100 m, with a weak inter-annual variability. It is known that this variability is consistent with local atmospheric forcing (wind stress, sea surface heating and evaporation rate), and the sea surface circulation, which is controlled by the bottom topography, the coastline and by mesoscale structures, such as the Algerian Eddies which can cause AW accumulation zones. This AW influences the water properties along the western Sardinian shelf with less salty waters (<37.0), and a density between 26.45 and 25.89 kg m⁻³ respectively in the years 2019 and 2020. The salinity near the bottom remained relatively constant at 38.0 during the three cruises. On the contrary, the water column of the casts along the central-northern coast showed a consistent impact by the AW coming from the centre of Algerian Basin, with a salinity core slightly higher (37.5).

Another interesting hydrodynamic phenomenon is the upwelling event along the north-western coast. It is observed in 2019, showing a rising of the isotherms from the bottom and forming an evident thermal front at the sea surface. The horizontal temperature anomaly reaches about +3 °C with respect to the surrounding waters.

The main driving force of the AW circulation on the southern and eastern Sardinian shelf is represented by the SESG. It appears in all ADT maps, and it is wide, encompassing two or three smaller cyclonic eddies, from observations during the cruises 2020 and 2021. Its shape and horizontal dimension can modify the AW stream flowing towards the Tyrrhenian basin, probably deviating an anti-clockwise part of AW to the Sardinian shelf. This is visible thanks to signatures of fresh AW with a salinity minimum of 37.5 between 35-40 m depth, particularly during the cruise in 2021 at the CTDs located on the central and south-eastern continental shelf.

From these analyses, in conclusion we can reasonably define that the water masses on the Sardinian shelf are represented by a mixing between the resident waters and the fresh AW which is characterized by a weak inter-annual variability. Its core ranges around 37.8 (the annual mean) with little difference between the west and east coast. Along the western coast the main dynamic spreading of AW is represented by the transport of AEs which affect the water column by less salty waters especially at the south-western and southern shelves. Here and on the eastern shelf the water properties depend on the dimension and position of the SESG, which can affect the coastal circulation and the water masses characteristics through the transport of modified AW from the Bifurcation Tyrrhenian Current (Sorgente et al., 2003).

5. Acknowledgments

The oceanographic data collection for this work was supported by the IDMAR (An Undersea Multidisciplinary Laboratory) Project funded by the Italian National Research Council and the Regional Operational Programme “Sicily 2014-2020” in the framework of the European Regional Development Fund (ERDF).

This work is part of the activities of the Spoke n. 1 (Mapping and monitoring actions to preserve marine ecosystem biodiversity and functioning) of the National Biodiversity Future Center (NBFC).

References

Artale, V., Astraldi, M., Buffoni, G., and Gasparini, G.P.: Seasonal variability of gyrescale circulation in the northern tyrrhenian sea. *J. Geoph. Res.*, 99 (C7), 14, 127–14 137, doi:10.1029/94JC00284, 1994.



- Barral, Q.-B., Zakardjian, B., Dumas, F., Garreau, P., Testor, P., and Beuvier, J.: Characterization of fronts in the Western Mediterranean with a special focus on the North Balearic Front, *Progr. Oceanogr.*, 197, 102636, doi:10.1016/j.pocean.2021.102636, 2021.
- 375 Benzohra, M., and Millot, C.: Characteristics and circulation of the surface and intermediate water masses off Algeria, *Deep Sea Res. Part I Oceanogr. Res.*, 42, 10, 1803-1830, doi:10.1016/0967-0637(95)00043-6, 1995.
- Chiocci, F.L., Budillon, F., Ceramicola, F., Gamberi, F., and Orrù, P.: Atlante dei lineamenti di pericolosità geologica dei mari italiani. Risultati del progetto MaGIC, CNR Eds., Roma. Italy, 262-341, 2021.
- Colas, F., McWilliams, J.C., and Capet, X., and Kurian, J.: Heat balance and eddies in the Peru-Chile current system, *Clim. Dyn.*, 39, 509–529, doi:10.1007/s00382-011-1170-6, 2012.
- 380 Cotroneo, Y., Aulicino, G., Ruiz, S., Pascual, A., Budillon, G., Fusco, G., and Tintoré, J.: Glider and satellite high resolution monitoring of a mesoscale eddy in the Algerian basin: Effects on the mixed layer depth and biochemistry, *J. Mar. Syst.*, 162, 73-88, doi:10.1016/j.jmarsys.2015.12.004, 2016.
- Escudier, R., Renault, L., Pascual, A., Brasseur, P., Chelton, D., and Beuvier, J.: Eddy properties in the western Mediterranean Sea from satellite altimetry and a numerical simulation, *J. Geophys. Res. Oceans*, 121, 3990–4006, doi:10.1002/2015JC011371, 2016.
- 385 Fuda, J.L., Millot, C., Taupier-Letage, I., Send, U., and Bocognano, J.M.: XBT monitoring of a meridian section across the western Mediterranean Sea. *Deep Sea Res. Part I Oceanogr. Res.*, 47, 2191–2218. doi: 10.1016/S0967-0637(00)00018-2, 2000.
- 390 García, M.J.L., Millot, C., Font, J., and García-Ladona, E.: Surface circulation variability in the Balearic Basin, *J. Geophys. Res.*, 99, 3285–3296, doi:10.1029/93JC02114, 1994.
- Iacono, R., Napolitano, E., Palma, M., and Sannino, G.: The Tyrrhenian Sea Circulation: A Review of Recent Work, *Sustainability*; 13(11), 6371, doi:10.3390/su13116371, 2021.
- Knoll, M., Borrione, I., Fiekas, H.-V., Funk, A., Hemming, M. P., Kaiser, J., Onken, R., Queste, B., and Russo, A.: Hydrography and circulation west of Sardinia in June 2014, *Ocean Sci.*, 13, 889–904, doi:10.5194/os-13-889-2017, 2017.
- 395 Krivosheya, V.G.: Water circulation and structure in the Tyrrhenian Sea, *Oceanology*, 23(2), 166– 171, 1983.
- Krivosheya, V.G., and Ovchinnikov, IM: Peculiarities in the geostrophic circulation of the waters of the Tyrrhenian Sea, *Oceanology*, 13, 822-827, 1973.
- Llinas, L., Pickart, R. S., Mathis, J. T., and Smith, S. L.: Zooplankton inside an Arctic Ocean cold-core eddy: Probable origin and fate, *Deep Sea Res. Part II Top. Stud. Oceanogr.*, 56, 17, 1290-1304, doi:10.1016/j.dsr2.2008.10.020, 2009.
- 400 Mancho, A. M., Hernández-García, E., Small, D., Wiggins, S., and Fernández, V.: Lagrangian Transport through an Ocean Front in the Northwestern Mediterranean Sea, *J. Phys. Oceanogr.*, 38, 1222–1237doi:10.1175/2007JPO3677.1, 2008.
- McGillicuddy, J.D. Jr.: Mechanisms of physical–biological–biogeochemical interactions at the oceanic mesoscale, *Annu. Rev. Mar. Sci.*, 8:1, 125-159, doi:10.1146/annurev-marine-010814-015606, 2016.
- 405 Millot, C.: Circulation in the western Mediterranean-Sea, *Oceanol. Acta*,10(2), 143–149, 1987
- Millot, C.: Circulation in the western Mediterranean Sea, *J. Mar. Syst.*, 20(1-4), 423–442, doi:10.1016/S0924-7963(98)00078-5, 1999.
- Millot, C.: Some features of the Algerian Current, *J. Geophys. Res.*, 90(C4), 7169–7176, doi:10.1029/JC090iC04p07169, 1985.
- 410 Millot, C., and Taupier-Letage, I.: Circulation in the Mediterranean Sea, In: *The Mediterranean Sea. Handbook of Environmental Chemistry*, Saliot, A. (eds), 5K. Springer, Berlin, Heidelberg, doi:10.1007/b107143, 2005.
- Obaton, D., Millot, C., d’Hieres, G. C., and Taupier-Letage, I.: The Algerian current: comparisons between in situ and laboratory data sets, *Deep Sea Res. Part I Oceanogr. Res.*, 47, 11, 2159-2190, doi:10.1016/S0967-0637(00)00014-5, 2000.



- 415 Olita, A., Ribotti, A., Fazioli, F., Perilli, A., and Sorgente, R.: Surface circulation and upwelling in the Sardinia Sea: A numerical study, *Cont. Shelf Res.*, 71, 95–108, doi:10.1016/j.csr.2013.10.011, 2013.
- Olita, A., Sparnocchia, S., Cusí, S., Fazioli, L., Sorgente, R., Tintoré, J., and Ribotti, A.: Observations of a phytoplankton spring bloom onset triggered by a density front in NW Mediterranean, *Ocean Sci.*, 10, 657–666, doi:10.5194/os-10-657-2014, 2014.
- 420 Perilli, A., Rupolo, V., and Salusti, E.: Satellite investigations of a cyclonic gyre in the central Tyrrhenian Sea (western Mediterranean Sea), *J. Geophys. Res.*, 100(C2), 2487–2499, doi:10.1029/94JC01315, 1995.
- Pessini, F., Cotroneo, Y., Olita, A., Sorgente, R., Ribotti, A., Jendersie, S., and Perilli, A.: Life history of an anticyclonic eddy in the Algerian basin from altimetry data, tracking algorithm and in situ observations, *J. Marine Syst.*, 207, 103346, doi:10.1016/j.jmarsys.2020.103346, 2020.
- 425 Pessini, F., Olita, A., Cotroneo, Y., and Perilli, A.: Mesoscale eddies in the Algerian Basin: do they differ as a function of their formation site?, *Ocean Sci.*, 14, 669–688, doi:10.5194/os-14-669-2018, 2018.
- Pinardi, N., Zavatarelli, M., Adani, M., Coppini, G., Fratiani, C., Oddo, P., Simoncelli, S., Tonani, M., Lyubartsevd, V., Dobricic, S., and Bonaduce, A.: Mediterranean Sea large-scale low-frequency ocean variability and water masses formation rates from 1987 to 2007: A retrospective analysis, *Prog. Oceanogr.*, 132, 318–332, doi:10.1016/j.pocean.2013.11.003, 2015.
- 430 Puillat, I., Taupier-Letage, I., and Millot, C.: Algerian Eddies lifetime can near 3 years, *J. Marine Syst.*, 31, 4, 245–259, doi:10.1016/S0924-7963(01)00056-2, 2002.
- Ribotti, A., Di Bitetto, M., Borghini, M., and Sorgente, R.: CTD profiles in western Sardinia (2000 - 2004), western Mediterranean, SEANOE, doi:10.17882/59867, 2019a.
- Ribotti, A., Perilli, A., Sorgente, R., and Borghini, M.: Hydrological profiles in the Mediterranean Sea (2002 - 2006), SEANOE, doi:10.17882/70340, 2019b.
- 435 Ribotti, A., Sorgente, R., Perilli, A., Cucco, A., Magni, P., and Borghini, M.: CTD profiles in the western and central Mediterranean between 2007 and 2020 from Italian cruises, SEANOE, doi:10.17882/87567, 2022.
- Ribotti, A., Puillat, I., Sorgente, R. and Natale, S.: Mesoscale circulation in the surface layer off the southern and western Sardinia Island in 2000–2002, *Chem. Ecol.*, 20:5, 345–363, doi:10.1080/02757540410001727963, 2004.
- 440 Rinaldi, E., Buongiorno Nardelli, B., Zambianchi, E., Santoleri, R., and Poulain, P.-M.: Lagrangian and Eulerian observations of the surface circulation in the Tyrrhenian Sea, *J. Geophys. Res.*, 115, C04024, doi:10.1029/2009JC005535, 2010.
- Schlitzer, R.: Ocean Data View, <https://odv.awi.de/>, 2023.
- Seyfried, L., Estournel, C., Marsaleix, P., and Richard, E.: Dynamics of the North Balearic Front during an autumn tramontane and mistral storm: air–sea coupling processes and stratification budget diagnostic, *Ocean Sci.*, 15, 179–198, doi:10.5194/os-15-179-2019, 2019.
- 445 Sorgente, R., Drago, A. F., and Ribotti, A.: Seasonal variability in the Central Mediterranean Sea circulation, *Ann. Geophys.*, 21, 299–322, doi:10.5194/angeo-21-299-2003, 2003.
- Taupier-Letage, I., and Millot, C.: Surface circulation in the Algerian basin during 1984, *Oceanolog. Acta, Océanographie pélagique méditerranéenne*, Ed. H. J. Minas and P. Nival, 79–85, 1988.
- 450 Taupier-Letage, I., Puillat, I., Millot, C., and Raimbault, P.: Biological response to mesoscale eddies in the Algerian Basin, *J. Geophys. Res.*, 108, C8, 3245, doi:10.1029/1999JC000117, 2003.
- Wunsch, C.: Where do ocean eddy heat fluxes matter?, *J. Geophys. Res.*, 104(C6), 13235–13249, doi:10.1029/1999JC900062, 1999.